DE GRUYTER OPEN

Curved and Layer. Struct. 2015; 2:183–193

Reseach Article

Open Access

Sachin Shrivastava and P.M. Mohite*

Redesigning of a Canard Control Surface of an Advanced Fighter Aircraft: Effect on Buckling and Aerodynamic Behavior

Abstract: A redesign of canard control-surface of an advanced all-metallic fighter aircraft was carried out by using carbon fibre composite (CFC) for ribs and panels. In this study ply-orientations of CFC structure are optimized using a Genetic-Algorithm (GA) with an objective function to have minimum failure index (FI) according to Tsai-Wu failure criterion. The redesigned CFC structure was sufficiently strong to withstand aerodynamic loads from stress and deflection points of view. Now, in the present work CFC canard structure has been studied for its buckling strength in comparison to existing metallic design. In this study, the existing metallic design was found to be weak in buckling. Upon a detailed investigation, it was revealed that there are reported failures in the vicinity of zones where initial buckling modes are excited as predicted by the finite element based buckling analysis. In view of buckling failures, the redesigned CFC structure is sufficiently reinforced with stringers at specific locations. After providing reinforcements against buckling, the twist and the camber variations of the airfoil are checked and compared with existing structure data. Finally, the modal analysis has been carried out to compare the variation in excitation frequency due to material change. The CFC structure thus redesigned is safe from buckling and aerodynamic aspects as well.

Keywords: canard; buckling; modal analysis; twist; camber; failure index; genetic-algorithm

*Corresponding Author: P.M. Mohite: Department of Aerospace Engineering, Indian Institute of Technology Kanpur, UP, India 208016, E-mail: mohite@iitk.ac.in, Tel: +91-512-2596024, Fax: +91-512-2597626
Sachin Shrivastava: Department of Aerospace Engineering, Indian Institute of Technology Kanpur, UP, India 208016

1 Introduction

The carbon fibre composites (CFC) are new generation materials with high strength to weight ratio, high fatigue strength and corrosion resistance over commercially available structural materials. Due to high strength to weight ratio, the replacement of metals with CFC laminates results in a great saving in terms of weight. The laminates are formed by stacking of laminae. Therefore, they can be formed to any shape easily, which is a definite advantage from the perspective of aircraft industry. The laying up of laminae can have many different possible combinations in composite materials and with each layup combination directional properties of the laminate varies. In [1] the redesign of an all-metallic advanced fighter aircraft canard control-surface using HexPLY® carbon fibre/epoxy composite IM7/8552 has been carried out. IM7/8552 is an epoxy based unidirectional carbon fibre composite material. This prepreg is widely used for manufacturing of major load carrying members like wing spar, bottom panel, longerons, etc. HexPLY® IM7/8552 has very good impact strength and is damage tolerant in numerous applications. IM7/8552 has 45% less weight density as compared to existing high strength aluminum alloys used in the current control surface structure [2]. By the virtue of difference in weight densities, about 12% weight reduction has been achieved in a design with the implication of HexPLY® IM7/8552 to the ribs and panels of control surface structure.

To optimize the redesigned structure of canard control surface a genetic algorithm (GA), as a non-traditional optimization procedure, was used. GAs were first developed by Holland [3] with an emphasis to use computers to design such systems which behave like nature, that is, systems should have self repair and self guidance characteristics. Later with the advent of computers, the concept became very popular to solve complex engineering problems where objective function is orthogonal in nature [4].

A box-beam model of a wing cross-section was studied by Carlos et al. [5] for variations of divergence and flutter

speeds with a change in the lamination sequences. Aeroelastic tailoring by the use of lamination parameters was optimized by Leon et al. [6]. They analyzed a composite wing subjected to aeroelastic effects and the resulting improvement in flutter speed by means of eigen frequency maximization. Leon et al. [6] initially developed a flat plate aeroelastic model and identified the eigen frequency responsible for the flutter. In next step, they have solved optimization problem to maximize specific eigen frequency with reinforcing fiber orientation as design variables. On the other hand, Kumar et al. [7] has carried out experiments and analysis using NASTRAN on a plate with and without slots on woven glass epoxy laminates for buckling behavior under in plane loading. They brought out the influence of length-to-thickness ratio, aspect ratio, fiber orientation in plies and the cut-out shapes on the buckling load. Guo [8] has carried out numerical and experimental studies to investigate the effect of reinforcement around cutouts on stress concentration and buckling behavior for carbon/epoxy laminates under shear loading. Based on the correlation established between numerical and experimental results Guo [8] suggested the best cutout scheme. Abramovich et al [9] brought out their experimental results on four torsion boxes by which they emphasized that the layup and geometry are major controlling factors to govern buckling load of the structure. Natarajan et al. [10] have studied the static bending and free vibration of thin and moderately thick laminated plates and demonstrated the effectiveness of the formulation through numerical examples.

Almeida and Awruch [11] in their work proposed a technique for the design and optimization of composite laminated structures using GA and finite element method (FEM). In their work they have considered composite shell under pressure and carried out stiffness maximization, which is an important parameter in aeroelasticity. Hassan et al. [12] analysed torsional vibrations of laminated composite beams with doubly symmetrical cross section using ANSYS 10.0. The reported results highlighted the effects of ply stacking sequences. Rajappan and Pugazhenthi [13] carried out a parametric study and brought out the effect of airfoil thickness variation on aeroelastic behavior for a wing made of laminated fibrous composites. Mohazzab and Dozio [14] presented a versatile and efficient modeling and solution framework for free vibration analysis of composite laminated cylindrical and spherical panels. They carried out modeling considering laminate as an equivalent single layer. The unified formulation of the equations of motion presented by them can be used for both thin and thick structures. Bachrach and Kodiyalam [15] suggested models to tailor the laminate sequences for the modal

frequencies in geometrically complex structures. It was shown that by using these models, the modal analysis-optimization design cycle time is reduced. Hariri et al. [16] deployed several piezoelectric patches bonded on system under study. By the application Kirchhoff-Love hypothesis, linear constitutive relations, plane stress formulation and Hamilton principle a two dimensional model was developed for the finite element method.

From the literature review it is seen that studies are mainly focused on plate type structures only and a limited work can be seen on much complex assemblies like wings and control surfaces. However, while considering changeover from metallic to CFC for the control surfaces or wings, it is very important that the aerodynamic shape (outer profile) should be free from local deformations which are likely due to buckling failure. Such local deformations on lifting surface can cause a loss of lift. Further, these local deformations cause global deviation in camber, which in turn affect the effectiveness of the control surface. Therefore, in redesign process care should be taken to check the acceptable deflections, local buckling and camber deformations. The loss of structural stiffness in such redesigns causes increased tip-deflections and local-buckling which has its direct implication on aeroelastic behavior of the control surface. In the present study a GA optimized redesign of CFC structure based on earlier work of authors [1] is further studied for its buckling and aerodynamic behavior along with the structural stiffness. An attempt has been made to quantify this behavior in terms of deflections and change in twisting angle of the airfoil shape.

In the following the basic features of the control surface studied are presented. Then the methodology used is explained in brief followed by the results obtained for an optimal structure under static loading in earlier work of authors. Then for this optimal design the buckling and aerodynamic behaviors have been studied in detail.

2 Internal structural arrangement and material details

The control surface structure under consideration consists of main-beam connected to longeron as a major load transferring member. This longeron is connected to transverse direction ribs to form the internal structure. On the ribs, the top and bottom panels are mounted and forms the required aerodynamic contour for the control surface as shown in Fig. 1(a). The ribs and panels of the structure are
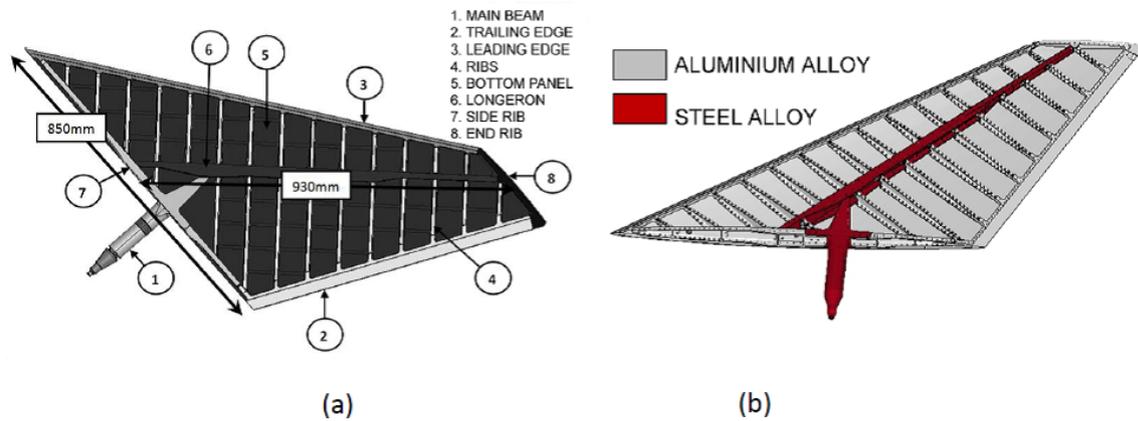
Figure 1: (a) Internal Structural Arrangement, (b) Materials of present structure

formed sheet metal members of high strength aluminum alloy of 1.5 mm and 2 mm sheet thickness, respectively.

Apart from ribs and panels, leading edge, trailing edge and side-ribs are made out of high strength aluminum alloy stampings. However, the main-beam and longeron material are machined components of high strength steel alloy. The Fig. 1(b) illustrates the types of materials used in the existing structure of the control surface.

3 Methodology adopted for redesign and optimization

The methodology adopted in the redesign of control surface is detailed in [1]. The approach used in the study is generic approach which can be implemented in any aerospace industry for typical control-surface structural member redesign and optimization. The approach followed is briefly presented in the following again:

1. The aerodynamic loading based on shear force and bending moment diagrams on the axis of longeron applied is used to obtain the pressure distribution on top and bottom face of the control surface.
2. The finite element based stress analysis results of existing metallic structure are generated for loading (see [1] for details). The results served as a basis for stresses and deflections to be maintained in the redesigned structure using CFC laminates.
3. The finite element model used in above analysis has used 12 layers and 16 layers laminates for ribs and panels, respectively. Three dimensional orthotropic mechanical properties of IM7/8552, as given in Table 1, are assigned to the model. The unknown prop-

erty G_{23} is calculated using three-phase concentric cylinder assemblage model of Christensen and Lo [17].

4. A GA is developed for the present optimization problem. The GA is guided by failure index value obtained using Tsai-Wu [18] failure criterion. The GA gives the optimized sequences for ply orientations for ribs and panels. The outer two layers in both ribs and panels are fixed to −45° and +45° as initial orientations. The laminates for ribs and panels are desired to be symmetric. Therefore, in the strings of GA there are only 4 and 6 design variables for ribs and panels, respectively. For some of the ribs, the obtained sequence was found to be unsafe under first-ply failure criterion. Therefore, their thicknesses were increased by adding two more layers. The optimal ply orientation sequences obtained after GA optimization procedure are shown in Fig. 3(a). The details of the study can be seen in [1].
5. Now, in the present study as a supplement to the work carried out in [1], study of buckling and aerodynamic behavior of the optimized CFC structure is carried out in detail.
6. The results obtained in bucking analysis are compared with the metallic structure buckling results.
7. The CFC canard design is sufficiently reinforced to achieve a safe design in buckling.

4 Finite element modeling

In this section the finite element modeling details, used in the buckling analysis model are presented. The model is developed using 2D planer elements for CFC components

considering the high cost of computation involved. However, components with isotropic material properties are discretized by 3D elements.

4.1 Elements and Meshing

The finite element discretization of control-surface has been carried out in HYPERMESH, which is based on a 3D-CAD model generated using CATIA. The solid model has been developed from the drawings available with the manufacturer for design of the subject part. The elements used in meshing are 4 noded 'quad' and 3 noded 'tria' elements for the CFC components, while the metallic parts are meshed with 4 noded tetrahedral elements. The panels and ribs are meshed on its mid surfaces and then assigned for laminate modeling with 0.125 mm thickness for each ply in ABAQUS. The parts are interconnected by 1D beam elements and distributed coupling elements at fasteners positions to form the assembly. The total number of nodes and elements present in the finite element model are 194567 and 413923, respectively. A convergence study with different number of elements and nodes has been carried out before using the above mentioned number of elements and nodes. However, the details of this study are not presented here.

Table 1: Mechanical Properties HexPLY® IM7/8552

0° Tensile Modulus (GPa)	E_{11}	163
Poisson's ratio	v_{12}	0.3
90° Tensile Modulus (GPa)	E_{22}	10
Transverse Shear Modulus	G_{23}	not known
0° Shear Modulus (MPa)	G_{12}	90
0° Tensile Strength (MPa)	X_t	2538
0° Compressive Strength (MPa)	X_c	1483
90° Tensile Strength (MPa)	Y_t	64
90° Compressive Strength (MPa)	Y_c	175
0° Inter Laminate Shear Strength (MPa)	Q	94
0° In Plane Shear Strength (MPa)	R	80
90° In Plane Shear Strength (MPa)	S	80

4.2 Control Surface Loading

The loading data obtained from designer is shown in Fig. 2. The loading diagram in the figure shows bending moment and shear force distribution over the longeron of the ca-

nard, along with a total design load of 10600 kgf on canard control surface. This design-load includes a design load factor of 1.5 over the limit-load. Hence, the limit load on the canard will be 7066 kgf. As a qualification test, control-surfaces are tested at 1.15 times of limit load [19] for its strength and buckling behavior. The structure is required to be safe under these testing conditions without any failure. Therefore, an analysis has been carried at test load condition to verify the design reliability.
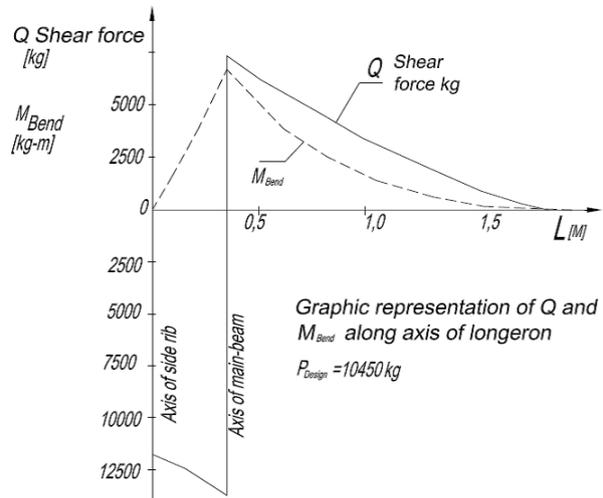

Figure 2: Bending Moment and Shear force diagram

4.3 Boundary Conditions

A bell crank lever (not shown) is mounted on main-beam via taper pins, which is connected to a hydraulic actuator. The hydraulic actuator, which is a part of flight control system, deflects the canard control surface as and when required as per flight control laws. During the operation, the canard control surface deflects according to the flight requirements. The flight control system sends signal to the hydraulic actuator to operate canard, which transfers motion to bell-crank. Based on above functional requirements, the boundary conditions in the finite element model are applied to simulate rotation of control surface about the axis of main beam and its fixity about bell-crank taper pin holes.

More details on the implementation can be seen in earlier work by authors [1].

5 Results and discussions

The ply orientations obtained after GA optimization procedure are depicted in Fig. 3(a) and the failure index (FI) plot for optimized design can be seen in Fig. 3(b). The Fig. 3(b) shows that the structure is safe with ply-orientation combinations with a maximum FI value of 0.97 at design loading, which is below unity for the safe design.

In the following the buckling and deflection analyses of the structures are presented.

5.1 Buckling Analysis of the Existing Structure

With the loads and boundary conditions discussed in Section 4, a finite element based buckling analyses [20] of the existing metallic structure and proposed CFC design structure have been carried out in ABAQUS 6.11 to evaluate its adequacy in buckling. The first (positive) buckling mode of existing metallic structure as obtained by analysis is shown in Fig. 4(a).

The finite element based buckling analysis results at the test load show that the existing metallic structure top-panel is failing due to buckling with an eigenvalue of 0.224, as illustrated in the Fig. 4(a). The result indicates that the existing metallic structure design is not safe in buckling. The analysis findings were confirmed by manufacturer and further five more failure cases in the vicinity of buckling hot spot, that is, in between rib 6 to rib 8 were reported. The reported failures are in different aircrafts after almost 1000 hours of flying. One of the failure cases due to buckling of top-panel in actual metallic structure is shown in the Fig. 4(b).

5.2 Buckling Analysis of CFC Design

The buckling analysis of CFC design indicates possible buckling of top-panel of CFC structure with an eigenvalue of 0.218 at the location shown in Fig. 5(a). This buckling mode is almost same as that of existing metallic structure design. In view of failures on existing metallic structure design, it is decided to add reinforcements to the top panel of CFC structure to strengthen the structure against buckling failure.

A possible design of aluminum alloy reinforcement proposed in the present analysis is shown in Fig. 5(b). The reinforcement suggested can be riveted to CFC top-panel from inside. For getting the final placement locations of the reinforcements, the buckling analysis has been carried out iteratively, with various placement combinations on or near to the buckling locations identified in each iteration analysis. The major steps involved in reaching the final configuration are outlined in Fig. 6.

The examination of Fig. 6 shows the shift of buckling location with incorporation of each stiffener. The placements of the stiffeners are shown on left side and the corresponding buckled shape is shown on right. After each step, the buckling eigenvalue magnitude is improvised but takes new position. The new position of hot-spot indicates the requirement of next stiffener to prevent buckling. The eigenvalue at the end of fifth step is 0.63, which can be brought to 1.0 by the incorporating few more stringers. However, after these reinforcements CFC design is almost 170% stronger than the existing metallic structure in terms of buckling. Therefore, the process is stopped here. In this process, additional weight penalty due to buckling reinforcement is 356 grams, which is just 0.8% of the weight of total weight of control surface. The placement of stiffeners in step 5 of the Fig. 6 indicates final locations of reinforcements on top-panel.

5.3 Deflection, Twist, CG and Camber Variation of Metallic and Reinforced CFC Structures

In the following subsections we present variation in deflection, twist and camber of the lifting surface. This study has been taken-up to understand how the control-surface will behave under the combination of bending and torsional loads due to aerodynamic lift-distribution.

5.3.1 Comparison of Deflections

The deflection of CFC as well as metallic canard is compared in the span-wise and chordwise directions. The span-wise deflection is an indicator of stiffness change. The results of z-direction deflection are presented in Fig. 7.

It can be seen from Fig. 7 that the tip deflection of canard has reduced by 14% with the use of CFC laminates and reinforcements. The decrement in canard tip deflection indicates stiffening of the structure with the replacement of aluminum by CFC laminated ribs and panels and reinforcements against buckling. Since, the stress levels after the use of CFC material are in acceptable range, therefore, the redesigned canard structure stiffening is acceptable.
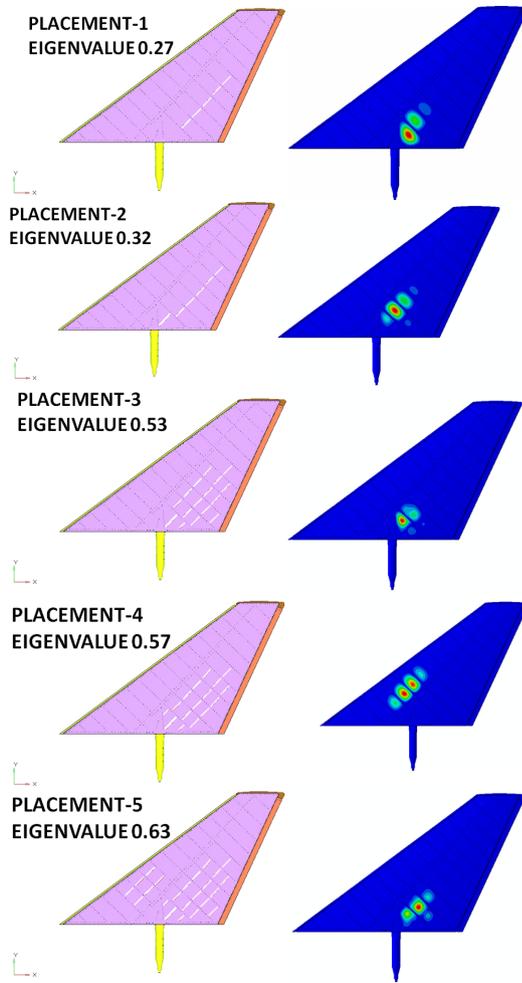
Figure 3: CFC Canard (a) Ply orientations (b) FI Index Plot

Figure 4: (a) Buckling Plot of Metallic Structure (b) Failure on Actual Structure

Figure 5: (a) Buckling Mode Plot of CFC Structure (b) A Proposed Buckling Reinforcement

5.3.2 Twist Comparison

In airfoil shapes, during operation, twisting occurs due to torsional load on structure. In the present case aerodynamically distributed load is a combination of bending as well as torsional loading. Therefore, twisting along with deflection is bound to happen, which will have direct implication on angle of attack that airfoil will experience during the flight. It is well known that a change in angle of attack leads to change in the lifting characteristics of

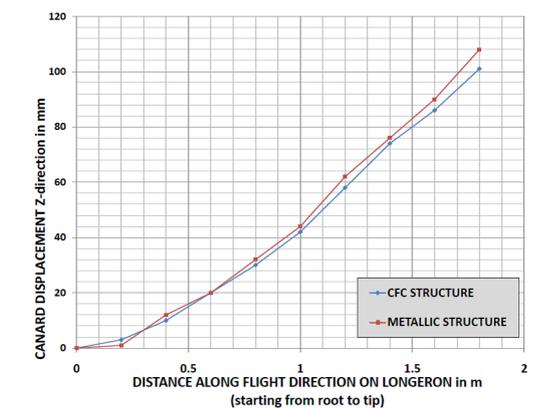**Figure 6:** Placement of Reinforcements to Increase Critical Buckling Load

Figure 7: Vertical Deflection on Axis of Longeron

the aerodynamic surface. Therefore, an attempt has been made to study the twisting under present loading conditions. To check the twisting of metallic and CFC structure, relative displacements between two extreme points, point-1 to point-4, as shown in Fig. 8(a) have been extracted out of analysis results. The calculation of twist angle based on coordinate data has been carried out by using Eq. 1 to Eq. 3 in the following.

From the coordinates given in Table 2, twist in metallic and CFC canard can be calculated using Eq. 1 to 3 as

$$\theta_i = \theta_{i(root)} - \theta_{i(tip)} \tag{1}$$

$$\theta_{i(root)} = \tan^{-1}\left(\frac{\Delta z_i - \Delta z_{i+1}}{\Delta x_i - \Delta x_{i+1}}\right) \tag{2}$$

$$\theta_{i(tip)} = \tan^{-1}\left(\frac{\Delta z_{i+1} - \Delta z_i}{\Delta x_{i+1} - \Delta x_i}\right) \tag{3}$$

where, Δ = displacement of individual structure
i =1, 2

From the results of Table 3, it can be seen that with change of material from metallic to CFC laminates, the twisting of the control surface is decreased by almost 16%. This indicates that the change of material to CFC laminates is acceptable in terms of twist of the structure.

5.3.3 CG change

An investigation has been made in the present work to determine shift in CG of the redesigned control surface structure, since the deflection of this part is always changing with time. So, with the use redesigned structure there should not be additional inertia forces due to change in CG position as shown in Table 4. Also, the study has been carried out to see the effect of shift of aircraft CG, which is found to be negligible (at the order 0.2% in AFT direction).

5.3.4 Camber Comparison

To study the variation in camber, airfoil section has been considered at three sections shown in Fig. 9(a). At these sections, nodes are selected and their x and z-coordinate data for the deformed metallic, CFC canard and un-deformed models are extracted. These data are plotted in Fig. 9(b) to Fig. 9(d). In the Fig. 9(b) through Fig. 9(d), the solid lines indicate un-deformed and deformed data of bottom-panel while dotted lines indicate un-deformed and deformed data of top panel. It can be seen that for all
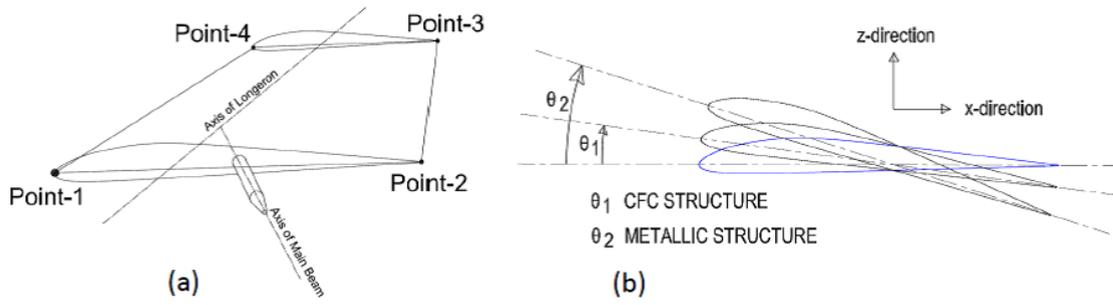
Figure 8: (a) Point locations for Twist data (b) Twisting angle for CFC and Metallic Structure

Table 2: Coordinates of CFC and Metallic Canard (All Coordinates are in mm)

	Model Coordinates			Deformed CFC Structure Coordinates			Deformed Metallic Structure Coordinates		
	x	y	z	x	y	z	x	y	z
Point1	26.52	15.0	0	26.4	15.9	−1.21	26.53	15.45	−1.11
Point2	1705.0	15.0	0	1705.0	14.80	15.66	1705	14.67	12.12
Point3	2302.4	1293.1	0	2302.8	1292.6	88.87	2304.4	1291.8	126.3
Point4	1833.7	1351.6	0	1834.1	1351.3	68.9	1833.9	1351.11	104.33

Table 3: Angle of Twist

	CFC Structure θ_1	Metallic Structure θ_2
at Root Rib	0.57°	0.45°
at Tip	2.44°	2.67°
Twist	1.86°	2.22°

the sections, camber deformation of CFC structure is less than that of metallic structure. Therefore, the aerodynamic shape deformation limits allowed for metallic structure are not exceeded by the CFC structure canard. This study gives section-wise information that there is no abrupt local deformation of the airfoil with the use of CFC laminates.

5.4 Modal Analysis

To compare mode shapes and excitation frequency of reinforced CFC design with the existing structure, modal analyses of structures have been carried out using finite element analysis. Section 5.4.1 presents generalized modal analysis. The results of the finite element modal analysis are presented in Section 5.4.2.

5.4.1 Eigenvalues and Eigenvectors of a Multi-degree Freedom System

Consider a simple multi-degree freedom system with mass matrix $\boldsymbol{M}$, stiffness matrix $\boldsymbol{K}$ and damping matrix $\boldsymbol{C}$ which is in excitation by time varying force vector $\boldsymbol{F}$. The equation of motion can be written as [21]

$$\mathbf{M}\ddot{X} + \mathbf{C}\dot{X} + \mathbf{K}\mathbf{X} = \mathbf{F} \tag{4}$$

For free vibration of un-damped system, Eq. 4 will reduce to

$$\mathbf{M}\ddot{X} + \mathbf{K}\mathbf{X} = \mathbf{0} \tag{5}$$

Eq. 5 is solved as eigenvalue problem,

$$\ddot{X} + \mathbf{A}\mathbf{X} = \mathbf{0} \tag{6}$$

where $\mathbf{A} = \mathbf{M}^{-1}\mathbf{K}$ and substituting, $\mathbf{X} = e^{i\omega}$ and $\omega^2 = \lambda$

$$(\mathbf{A} - \lambda.\mathbf{I})\,\mathbf{X} = 0 \tag{7}$$

where, λ =Eigenvalues and $\mathbf{X}$ = Eigenvectors

5.4.2 Modal Analysis of Metallic Structure and CFC Final-Design

To compare the effect of using CFC material for ribs and panels along with buckling reinforcements on the stiffness

Table 4: CG shift [Reference is point-1 of Fig. 8(a)]

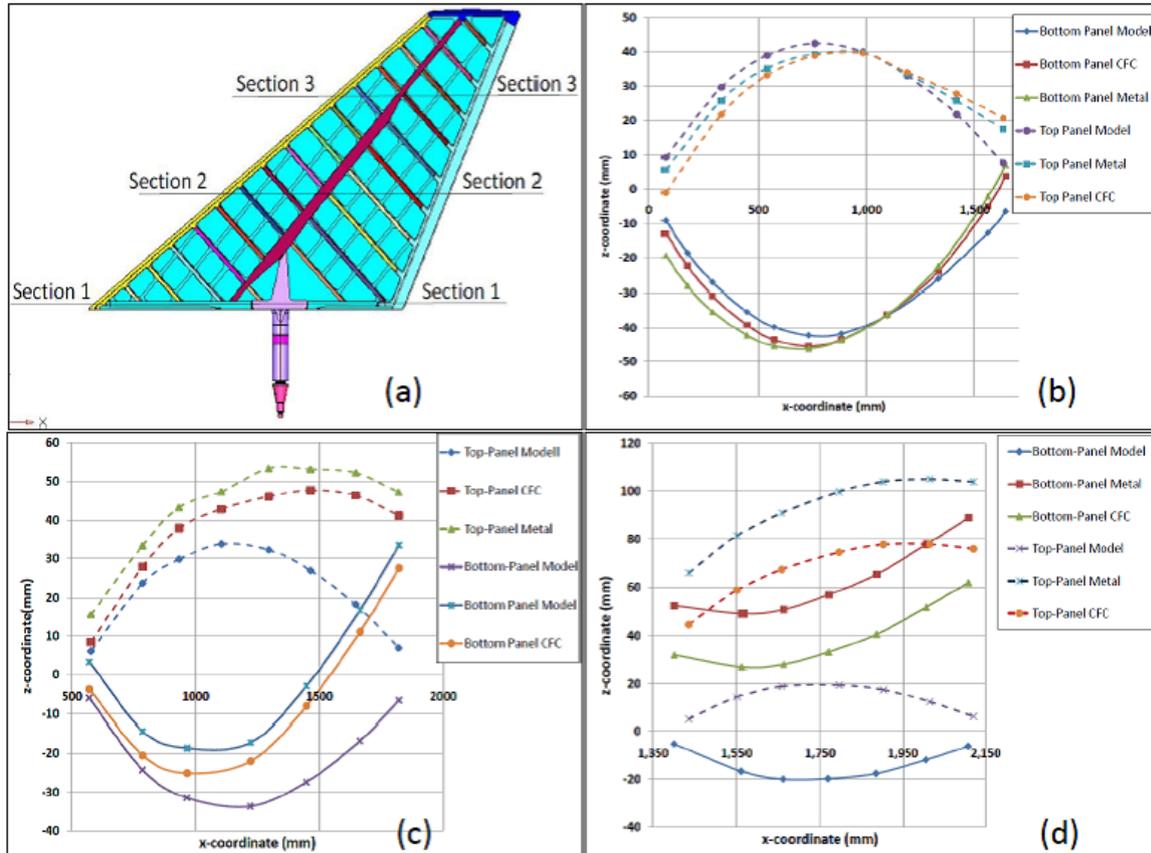|	Existing Structure	Re-designed CFC Structure	% change
+x-direction (along flight direction)	−653.4	−654.2	−0.12
+y-direction (towards wing tip)	156.2	154.3	+1.21
+z-direction (vertically upwards)	1.22	1.24	−1.63

Figure 9: (a) Sections of Camber and Deformations at Camber Section (b) 1, (c) 2, (d) 3

of the structure a modal analysis of metallic as well as CFC structure has been carried out. From the modal analysis the frequency for mode excitation and mode shapes are extracted. The results of modal analysis for the first five mode shapes along with their excitation frequencies are presented in Fig. 10. The first part of each figure is for CFC structure and later part is for metallic structure. Table 5 shows modal frequencies of the first five modes.

A comparative study of natural-frequency for mode excitation of metallic structure, CFC structure and CFC structure with reinforcements against buckling is carried out from the frequency plots of the first five modes and is shown in Fig. 11. This study of mode shapes and natural-frequency for initial modes, that is, vertical bending, in-plane bending and torsion mode indicates that present layer orientation combination is adding stiffness in longitudnal direction of canard. However, there is reduction in modal frequency when structure is vibrating in mode-2. This indicates reduction in structural stiffness in chordwise direction. In view of this analysis, if significant variations in frequency are encountered while redesign of structure, one can incorporate layers with fibers orientation in chordwise, i.e. 90° direction to bring back frequency of the particular mode in acceptable range. As a second option, one or two layers of 0° orientations can also be changed to 90° direction with a check on FI value. Similarly, the mode-3 results indicate that addition of layers in ±45° direction can be done to add stiffness in torsion. However, in present structure comparative study of mode excitation for the present structure does not show signifi-

Table 5: Modal Frequencies for CFC and Metallic Structure

Mode	Frequency	
	CFC Structure	Metallic Structure
Mode-1: Vertical Bending	26.31	23.13
Mode-2 : Horizontal (In-plane) Bending	39.16	44.88
Mode-3 : Torsion Mode	56.81	69.55
Mode-4 : Vertical Bending 2nd Mode	86.68	81.61
Mode-5 : Torsion 2nd Mode	93.79	101.6
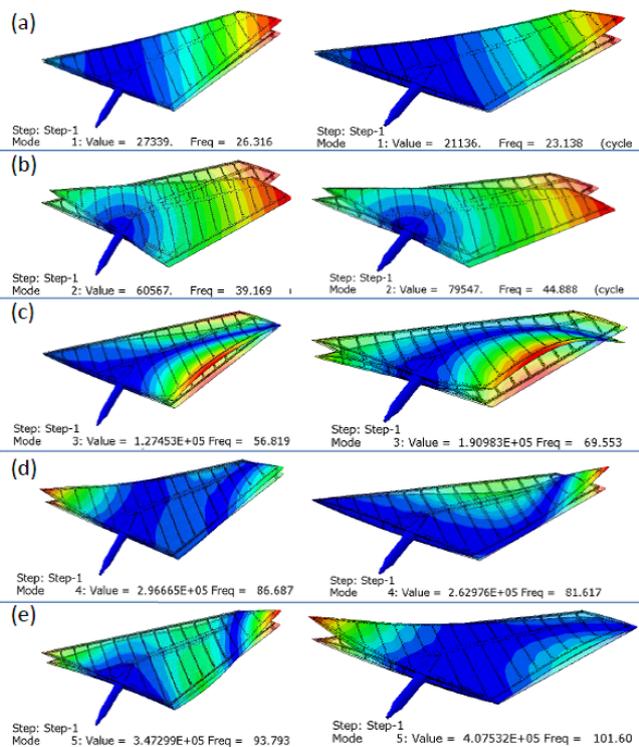
Figure 10: Mode Shapes CFC and Metallic Structure: (a) Mode 1, (b) Mode 2, (c) Mode 3, (d) Mode 4 and (e) Mode 5

cant variation mode shape and corresponding frequencies are shown in Fig. 11. The variation in mode shape and frequency at higher frequency can be accepted, since high energy is required to excite these modes. Moreover, it can be seen from the results that natural frequencies are well separated also (that is, no two frequencies are closer by at least 10 Hz). Therefore, the present structural results are good from flutter point of view also.
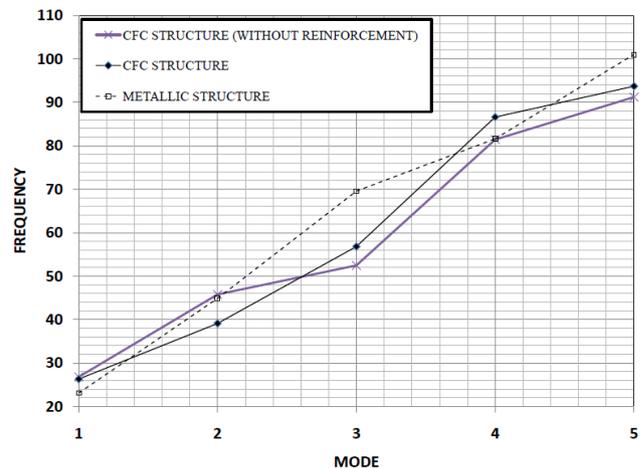
Figure 11: Mode Shape Excitation Frequency Plot

6 Conclusions

An all metallic canard structure is redesigned and optimized and in its new design the ribs and panels are replaced by unidirectional fibrous laminates. In the earlier work by authors this redesign and optimization was carried for fail safe design with Tsai-Wu first-ply criterion. Further, the deflections predicted under the design load were within limits. A GA was developed to carry out optimization. The GA string was developed with 4 and 6 design variables for ribs and panels, respectively in such a way that the resulting laminates are symmetric.

The redesigned structure needs to be analyzed for the buckling and aerodynamic behavior. The buckling and aerodynamic behaviour is important from performance point of view as a slight disturbance in aerodynamic behaviour can cause significant difference in control laws. Therefore, for the optimized structure a buckling analysis has been carried out in the present study. The analysis of the optimized structure has been carried out using ABAQUS 6.11. The key points that can be concluded from these analyses results are listed below.

1. The buckling analysis of existing metallic structure shows eigenvalue as 0.224 only, which indicates that existing design needs a detailed review from buckling point of view.

2. The failure location as indicated by manufacturer in existing design is in the vicinity of initial buckling modes shown by the analysis carried out. This indicates that the reported failures are likely due to the buckling of the structure.

3. In view of buckling failures on metallic design, the proposed CFC design is reinforced against buckling in steps. The addition of these reinforcements added 356 gm of additional weight, which is 0.8 % of total weight of the canard.

4. After reinforcements, CFC design is 1.7 times more reliable in terms of buckling compared to existing metallic structure design.

5. The redesigned CFC structure with reinforcements is within acceptable limits when compared for deflections, twisting, CG and camber variations.

6. The modal analysis shows a good correlation in its initial three modes, but the 4th and 5th modes were slightly changed, with a maximum of 8% variation in frequencies.

7. The modal analysis gives a fair idea on addition and removal of layers along with fiber orientations of additionally required or surplus available layers from stiffness point of view.

Conflict of Interest:

Declared none.

References

[1] Shrivastava S., Mohite P.M., Design and optimization of a composite canard control surface of an advanced fighter aircraft under static loading, *Curved Layer. Struct.*, **2015**, 2, 91-105.

[2] Hexel Composites, Product Data of HexPlyIM7/8552 Carbon Fiber Epoxy matrix laminate, 2013, http://www.hexcel.com/Resources/DataSheets/Prepreg-Data-Sheets/8552_eu.pdf

[3] Holland J.H., Complex adaptive systems, *Daedalus*, **1992**, *121*, 17-30.

[4] Balaji C., Madadi R.R., Optimization of the location of multiple discrete heat sources in a ventilated cavity using artificial neural networks and micro genetic algorithm, *Int. J. Heat Mass Transfer*, **2008**, *51*, 2299-2312.

[5] Carlos E.S.C., Hodges H.D., Patil J.M. Aeroelastic analysis of composite wings, In: *Proceedings of 37th Structures, Structural Dynamics and Materials Conference* (15-17 April 1996, Salt Lake City, Utah, USA) *AIAA J*, **1996**, 1-11.

[6] De Leon D.M., de Souza C.E., Fonseca J.S.O., da Silva R.G.A., Aeroelastic tailoring of composite plates through eigenvalues optimization, *Mecánica Computacional*, **2010**, *29*, 609-623.

[7] Kumar M.M., Jacob C.V., Lakshminarayana N., Puneeth B.M., Nagabhushana M., Buckling analysis of woven glass epoxy laminated composite plate. *Am. J. Eng. Res.*, **2013**, *2*, 33-40.

[8] Guo S.J., Stress concentration and buckling behavior of shear laded composite panel with reinforced cutouts, *Compos. Struct.*, **2007**, *80*, 1-9.

[9] Abramovich H., Weller T., Bisagni C., Buckling behavior of composite laminated stiffened panels under combined shear-axial compression, *J. Aircraft*, **2008**, *45*, 402-413.

[10] Natarajan S., Ferreira A.J.M., Nguyen-Xuan H., Analysis of cross-ply laminated plates using isogeometric analysis and unified formulation. *Curved Layer. Struct.*, **2014**, *1*, 1-10.

[11] Almeida F.S., Awruch A.M., Design optimization of composite laminated structures using genetic algorithms and finite element analysis, *Compos. Struct.*, **2009**, *88*, 443-454.

[12] Hassan G.A., Fahmy M.A., Goda I.M., The effect of fiber orientation and laminate stacking sequences on the torsional natural frequencies of laminated composite beams, *J. Mech. Design Vib.*, **2013**, *1*, 20-26.

[13] Rajappan R., Pugazhenthi V., Finite element analysis of aircraft wing using composite structure. *Int. J. Eng. Sci.*, **2013**, *2*, 74-80.

[14] Mohazzab A.H., Dozio L., Prediction of natural frequencies of laminated curved panels using refined 2-D theories in the spectral collocation method, *Curved Layer. Struct.*, **2015**, *2*, 1-14.

[15] Bachrach W., Kodiyalam S., Effective mechanical properties strategy for modal analysis and optimization of composite structures, *Compos. Eng.*, **1995**, *5*, 1-7.

[16] Hariri H., Bernard Y., Razek A., A two dimensions modeling of non-collocated piezoelectric patches bonded on thin structure, *Curved Layer. Struct.*, **2014**, *2*, 2353-7396.

[17] Christensen R. M., Lo K.H., Solutions for effective shear properties in three phase sphere and cylinder models, *J. Appl. Mech. Phys. Solids*, **1979**, *27*, 315-330.

[18] Tsai S.W., Wu E.M., A general theory of strength for anisotropic materials, *J. Compos. Mat.*, **1971**, *5*, 58-80.

[19] MIL-STD-8591, Airborne Stores, Suspension Equipment and Aircraft-store Interface (Carriage Phase), Department of Defense USA, Design Criteria's for Standard, 12th Dec 2009.

[20] Shames I.H., Clive D., Energy and Finite Element Methods in Structural Mechanics SI Unit Edition, Taylor & Francis, New York, 1991.

[21] Thomson W.T., Theory of Vibration with Application 4th Edition, Stanley Thrones Publishers Ltd, 1998.